# Long-range multipolar potentials of the 18 spin-orbit states arising from the C($^3$P) + OH(X$^2\Pi$) interaction

Béatrice Bussery-Honvault*

*Institut UTINAM, UMR CNRS 6213,*

*Université de Franche-Comté, 25030 Besançon cedex, France*

Fabrice Dayou

*LERMA, UMR 8112, Observatoire de Paris-Meudon, 92195 Meudon cedex, France*

Alexandre Zanchet

*Institut de Physique de Rennes, UMR CNRS 6251,*

*University Rennes 1, 35042 Rennes Cedex, France*

(Dated: September 26, 2008)

## Abstract

We present the multipolar potentials at large intermolecular distances for the 18 doubly-degenerate spin-orbit states arising from the interaction between the two open-shell systems, C($^3$P) and OH(X$^2\Pi$). With OH fixed at its ground vibrational state averaged distance $r_0$, the long-range potentials are two-dimensional potential energy surfaces (PESs) that depend on the intermolecular distance $R$ and the angle $\gamma$ between $R$ and $r$. The 18 $\times$ 18 diabatic potential matrix elements are built up from the perturbation theory up to second order and from a two-center expansion of the coulombic interaction potential, resulting in a multipolar expansion of the potential matrix expressed as a series of terms varying in $R^{-n}$. The expressions for the long-range coefficients of the expansion are explicitly given in terms of monomer properties such as permanent multipole moments, static and dynamic polarizabilities. Accurate values for the monomer properties are used to properly determine the long-range interaction coefficients. The diagonalization of the full 18 $\times$ 18 potential matrix generates adiabatic long-range PESs in good agreement with their *ab initio* counterparts.

* Author to whom correspondence should be adressed; e-mail: beatrice.honvault-bussery@univ-fcomte.fr

## I. INTRODUCTION

Reactions with OH are relevant to the chemistry of planetary atmospheres and interstellar medium. Indeed, the hydroxyl radical reacts with a lot of compounds and, despite its very short lifetime, it acts as a cleaner of the Earth atmosphere since it can transform active species into inactive ones, and inversely. Nevertheless, there are only few experimental results for this class of reactions as experiments with two radicals are difficult to perform or impossible to achieve in practice [1–4]. So theoretical studies are needed in order to predict rate constants or to confirm the measured ones, in particular at low temperatures of interest for the interstellar dense clouds (10 K - 30 K). In radical-radical reactions, there often are no barrier to reaction for optimal angles of approach, and, hence, low energy collisions generally assume great importance. In such a case, an accurate knowledge of the long-range potential surfaces is crucial to get a proper description of the dynamics at low temperatures. At large separations, the interaction potential between two neutral systems can be expressed in terms of inverse powers of the intermolecular distance, $R$. The long-range interaction coefficients of such an expansion are a valuable tool for predicting very accurately the asymptotic behavior of the PESs. For open-shell systems the situation is further complicated as the adiabatic states correlate to degenerate states of the fragments (such as the atomic $P$ and diatomic $\Pi$ states in the present case), giving rise generally to a breakdown of the Born-Oppenheimer (BO) approximation. A solution to this problem was suggested by Smith[3], who proposed the concept of diabatic states, linear combinations of adiabatic states. The introduction of diabatic states is at the expense of dealing with a non-diagonal PES matrix.

Fine structure splitting can either greatly control the kinetics of such reactions, as transitions may occur among the multiple states correlating to different reactant fine-structure levels. Indeed, for exoergic reaction driven by a barrierless PES, the influence of fine-structure populations on reactivity is highly dependent on the adiabaticity of the collision. However, in our previous studies [5–7] and in the vast majority of reaction dynamics, the assumption is made that transitions do not occur between states correlating with different fine-structure levels. Populations are assumed to partition adiabatically onto reactive or non reactive PESs as the reactants approach each other and so, thermal rate constants include this effect through a simple multiplicative factor corresponding with the probability of initiating a collision on a given reactive PES. The behavior of rate constants with the

temperature is then greatly modified according to this Maxwell-Boltzmann factor as can be seen on Fig.4 of Ref.[5]. In particular, the role of fine structure effects in the C+OH reaction will be important in nonthermal environments such as diffuse interstellar clouds.

Either, the dynamics of ultracold collisions is governed by long-range interactions, as the intermolecular forces between the reactants are much larger than their initial kinetic energy. Therefore, there is a need to precisely describe the interaction potentials at the very long range of the intermolecular distance. Since the long-range interactions are determined by intrinsic properties of each reactive specie, such as the permanent multipole moments and polarizabilities, these quantities must be evaluated with extreme accuracy.

The interaction between an open-shell (such as OH) and a closed shell system is already an interesting case of study, as the closed-shell system lifts the degeneracy of the open-shell ($^2\Pi$ for OH) electronic state [8–12]. The interaction between two open-shell systems is even more challenging due to the size increase of the interaction matrix, and scarce works exist in such cases [8, 13, 14]. Indeed, the interaction of C($^3$P)+ OH($X^2\Pi$) gives rise to 18 doubly degenerate states when fine-structure levels are considered (12 electronic states if spin-orbit couplings are neglected) and long-range studies of open-shell atom + OH systems have been investigated, to our knowledge, at the electrostatic energy level only[8] or within a state averaged approximation [14].

We are presently interested in such radical-radical long-range potentials and their non-adiabatic couplings in the special case of collision between a ground state carbon atom C($^3$P) and a ground state hydroxyl radical OH($X^2\Pi$). This reactive collision is a source of carbon monoxide in the universe (interstellar medium, atmospheres, comets, ...) and a sink of the hydroxyl radical. Recently, a global PES has been built for the ground $X^2A'$ state[5] of C+OH based on the multi-reference configuration interaction (MRCI) method, including the Davidson correction, with Dunning aug-ccpVQZ basis sets. No barrier has been observed in the entrance channel of the PES. Based on this PES, quasiclassical dynamics studies have furnished estimations of cross-sections and rate constants of the C($^3$P) + OH($X^2\Pi$) $\rightarrow$ CO($X^1\Sigma^+$) + H($^2$S) reaction [6, 7].

We present in Sec.II the formalism to evaluate the electrostatic, dispersion and induction energies of the doubly-degenerate 18 long-range states of C($^3$P) + OH($X^2\Pi$) including the monomer spin-orbit splittings and in Sec III, the results of the calculations as well as a discussion of these results. We conclude the paper in Sec IV.

## II. THE C+OH POTENTIAL ENERGY SURFACES

The potential energy surfaces associated with the C($^3$P) + OH(X$^2\Pi$) system have been studied by means of *ab initio* quantum chemistry calculations [15], globally for the X$^2A'$ ground state [5] and the first excited $^{2,4}A''$ [16] states, and in the region of the entrance channel for the $^{2,4}A'$ [16] states. To date, none of the latter PESs has included an accurate description of the long-range part. Those long range potentials are described here following the perturbation theory up to second order and using a two-center expansion of the intermolecular coulombic potential, leading to a series of terms varying in $1/R^n$. The first order perturbation will be described in first approximation by quadrupole-dipole and quadrupole-quadrupole interactions, giving rise to potential matrix elements varying in $1/R^4$ and $1/R^5$ respectively. The second order perturbation, leading to the dispersion and induction energies involving induced multipole moments, will be truncated to terms in $1/R^6$. Taking into account the 36 fine structure states dissociating into C($^3$P) + OH(X$^2\Pi$) results in a 36×36 diabatic potential matrix, whose diagonalization leads to 18 doubly-degenerate adiabatic PESs. To describe the long-range part of such an atom-diatom system we employed the usual set of Jacobi coordinates, i.e. the intermolecular separation $R$ between carbon atom and the OH center-of-mass, the intradiatomic distance $r$, and the angle $\gamma$ between the two vectors $\mathbf{R}$ and $\mathbf{r}$. The $(R, r, \theta)$ set of coordinates previously defined in Ref. [5] relates with the present one by $\gamma = \pi - \theta$ and thus, in present work, $\gamma$=0° corresponds to linear OHC and $\gamma$=180° to linear COH. The OH internuclear distance $r$ has been kept fixed at its ground vibrational state averaged distance $r_0$, and, thus, we are actually dealing with two-dimensional PESs matrix elements, depending on $R$ and $\gamma$ only.

### A. Formalism for the electrostatic energy

The electrostatic energy between two interacting systems A (carbon atom) and B (hydroxyl radical), given by the first order of the perturbation theory, writes

$$E^{(1)} = \langle \Psi_{00} \, | \hat{V}_{ab} \, | \Psi_{00} \rangle \tag{1}$$

where $\Psi_{00} = \Psi_a^0 \Psi_b^0$ is the product of the C($\Psi_a^0$) and OH($\Psi_b^0$) ground state electronic wavefunctions of each unperturbed system, $\hat{V}_{ab}$ the coulombic interaction potential operator, and

A and B are considered far enough apart that the overlap between their wavefunctions can be neglected. In that case, the multipole expansion of $\hat{V}_{ab}$ writes

$$\hat{V}_{ab} = \sum_{l_a l_b} \frac{1}{R^{l_a+l_b+1}} \sum_{m=-l_<}^{l_<} g_m(l_a, l_b)\ \hat{Q}_{l_a}^{m}\ \hat{Q}_{l_b}^{-m} \tag{2}$$

where $l_<$ =min$(l_a, l_b)$ and the factor $g_m(l_a, l_b)$ writes

$$g_m(l_a, l_b) = (-1)^{l_a}\sqrt{2L_{ab}+1} \begin{pmatrix} 2L_{ab} \\ 2la \end{pmatrix}^{1/2} \begin{pmatrix} l_a & l_b & L_{ab} \\ m & -m & 0 \end{pmatrix} \delta_{L_{ab},l_a+l_b} \tag{3}$$

where $\binom{a}{b}$ is a binomial coefficient. The multipole moment operators $\hat{Q}_l^m$ associated with each monomer are defined such as

$$\hat{Q}_l^m = \sqrt{\frac{4\pi}{2l+1}} \sum_{i=1}^{N} q_i r_i^l Y_l^m(\theta, \phi) \tag{4}$$

where $N$ equals the number electrons plus the nucleus of each monomer. In the above equations, we have aligned the intermolecular axis $\mathbf{R}$ along the $z$-axis of the space-fixed (SF) coordinate frame so that the body-fixed (BF) $z$-axis and the SF $z$-axis coincides. The multipole moment operators $\hat{Q}_l^m$ are defined in the SF coordinate frame, $m$ being the projection of the $l$ angular momentum along the SF $z$-axis and $\hat{\omega} = (\phi, \theta, 0)$ defines the set of Euler angles of each monomer in the SF frame. Since we are dealing with a triatomic system, we furthermore choose the $xz$-plane of the BF frame to be coincident with the $xz$-plane of the SF frame so that $\phi_a = \phi_b$=0.

The zero-order ground state wavefunction of the OH diatom is labelled $|\Psi_0(\mathrm{OH})\rangle = |\Lambda, \Sigma\rangle = |\pm 1, \pm\frac{1}{2}\rangle$ or $|\mp 1, \pm\frac{1}{2}\rangle$, where $\Lambda$ and $\Sigma$ are the projection of the molecular orbital and spin angular momenta along the OH intradiatomic axis $\mathbf{r}$, respectively. For a diatomic molecule, they are good quantum numbers that lets define $\Omega = \Lambda + \Sigma$ as the projection of the total angular momentum along the intradiatomic axis.

The zero-order ground state wavefunction of the carbon atom is labelled $|\Psi_0(\mathrm{C})\rangle = |LSM_LM_S\rangle$ in the $LS$ coupling case (if spin-orbit coupling is neglected), and $|JM_J\rangle$ in $JJ$ coupling case (when spin-orbit coupling is accounted for). $M_L$ is the projection of the $L$ electronic orbital momentum of the carbon atom along the BF $z$-axis, $S$ and $M_S$ are the total spin and spin projection along the BF $z$-axis, $J$ is the total $\mathbf{L}$+$\mathbf{S}$ angular momentum

and $M_J$ its projection along the BF $z$-axis. The $|JM_J\rangle$ (coupled) basis states are related to the $|LSM_LM_S\rangle$ (uncoupled) ones by

$$|JM_J\rangle = \sum_{M_L M_S} |LSM_LM_S\rangle \langle LSM_LM_S \mid JM_J\rangle \tag{5}$$

where $\langle LSM_LM_S \mid JM_J\rangle$ is a Clebsch-Gordan coefficient and $M_J = M_L + M_S$. The eigenfunctions $|JM_J\rangle$ and $|LSM_LM_S\rangle$ have been tabulated for the $(p^2)^3P$ state of carbon atom by Gentry and Giese (see Table 3 of Ref.[17]).

The multipole moments $\hat{Q}_l^m$ of Eq. 2 are defined with respect to a SF frame. In order to get potential matrix elements with an explicit $\gamma$ dependence, it is preferable to deal with multipole moments $\hat{q}_l^{m'}$ defined relative to molecular-fixed axis. Let $\hat{\omega} = (\phi_b, \gamma, 0)$ be the Euler angles of the OH intradiatomic axis $\mathbf{r}$ relative to the SF frame. In such a case, the multipole moment operators defined relative to the SF and OH bond axis are related by:

$$\hat{Q}_l^m = \sum_{m'} \hat{q}_l^{m'} \ \left[D^l_{mm'}(\hat{\omega})\right]^* \tag{6}$$

where $D^l_{mm'}(\hat{\omega})$ is the Wigner rotation matrix between the SF and molecular-fixed frames. Furthermore, since $\phi_b$=0, we have $D^l_{mm'}(0,\gamma,0) = d^l_{mm'}(\gamma)$, where $d^l_{mm'}(\gamma)$ is a reduced Wigner rotation matrix. Using Eqs. 2 and 6, the electrostatic energy expressed in the $|JM_J\rangle\,|\Lambda,\Sigma\rangle$ diabatic basis set then writes:

$$E_{\rm elec}^{JM_JJ'M'_J\Lambda\Sigma\Lambda'\Sigma'} = \sum_{l_a l_b} \frac{1}{R^{l_a+l_b+1}} g_m(l_a,l_b) \,\langle JM_J \,|\hat{Q}^m_{l_a}\,|J'M'_J\rangle\,\langle\Lambda|\,\hat{q}^{m'}_{l_b}\,|\Lambda'\rangle\, d^{l_b}_{-mm'}(\gamma)\delta_{\Sigma\Sigma'} \tag{7}$$

where $\langle JM_J \,|\hat{Q}^m_{l_a}\,|J'M'_J\rangle$ and $\langle\Lambda\,|\hat{q}^{m'}_{l_b}\,|\Lambda'\rangle$ represent the $2^{l_b}$-pole of C and OH, respectively. From the Wigner-Eckart theorem, it follows that the latter matrix elements are zero unless $m = M_J - M'_J$ and $m' = \Lambda - \Lambda'$.

The 4×4 matrix $\langle\Lambda\Sigma\,|\hat{q}^{m'}_{l_b}\,|\Lambda'\Sigma'\rangle$ for OH reduces to a 2×2 doubly-degenerate $\langle\Lambda\,|\hat{q}^{m'}_{l_b}\,|\Lambda'\rangle\,\delta_{\Sigma,\Sigma'}$ matrix due to the $\delta_{\Sigma,\Sigma'}$ factor. Diagonal elements ($\Lambda - \Lambda' = 0$) will depend on $\hat{q}^0_1$(OH)=$\hat{\mu}_{\rm OH}$ and $\hat{q}^0_2$(OH), the dipole and quadrupole moment operators of OH, respectively (note that in Ref. [8], $Q_{\rm OH} = 2q^0_2({\rm OH})$ is used instead). For diatomics in a $\Pi$ state, $\Lambda - \Lambda' = 0, \pm 2$, so that matrix elements of $\hat{q}^{\pm 1}_l$ are all zero. Extra-diagonal matrix elements ($\Lambda - \Lambda' = \pm 2$) will depend on $\hat{q}^{\pm 2}_2$(OH) only (noted $Q_c$(OH) in Ref. [8]). An explicit

$\gamma$-dependence of the 2×2 potential matrix is given by Eq.(14) of Ref. [8]. But, it is worth to note that the definition of the $\hat{Q}_l^m$(GW) multipole moments is not the same as that given by Eq. 4 of present work. Both definitions are related by

$$\hat{Q}_l^m(\text{Eq. (4)}) = (-1)^{m-|m|}\sqrt{\frac{(l-m)!}{(l+|m|)!}}\hat{Q}_l^m(\text{GW}). \tag{8}$$

The $\langle JM_J\,|\hat{Q}_{l_a}^m\,|J'M'_J\rangle$ matrix elements for carbon atom build up a 9×9 matrix. Since $Q_1^m$ dipole moments are zero for atoms, the first non zero permanent multipole moments of carbon will be the quadrupole moment ($la = 2$). According to Graff and Wagner [8], the $\langle JM_J\,|\hat{Q}_2^m\,|J'M'_J\rangle$ matrix elements can be expressed as proportional to the quantity $Q_2$(C)= $2\langle L0\,|\hat{Q}_2^0\,|L0\rangle$. We present those relations in Appendix A for the $\langle JM_J\,|\hat{Q}_2^m\,|J'M'_J\rangle$ matrix elements of carbon, with $m$=0,1 and 2, as they differ slightly from the ones of Ref. [8]. Using Eq. 5, the electrostatic energies of Eq. 7 can also be rewritten as a function of the $\langle LM_L\,|\hat{Q}_{l_a}^m\,|LM'_L\rangle$ matrix elements as

$$\begin{aligned} E_{\text{elec}}^{JM_JJ'M'_J\Lambda\Sigma\Lambda'\Sigma'} &= \sum_{l_al_b}\frac{1}{R^n}\sum_{M_LM_SM'_LM'_S}\langle LSM_LM_S\mid JM_J\rangle\langle LSM'_LM'_S\mid J'M'_J\rangle \\ &\times\delta_{M_SM'_S}\delta_{\Sigma\Sigma'}\,{}^{ii'jj'}V_{nl_bM_aM_b}^{\text{elec}}\,d_{-M_aM_b}^{l_b}(\gamma) \end{aligned} \tag{9}$$

where the electrostatic interaction coefficients ${}^{ii'jj'}V_{nl_bM_aM_b}^{\text{elec}}$ write

$${}^{ii'jj'}V_{nl_bM_aM_b}^{\text{elec}} = g_m(l_a,l_b)\,\langle LM_L\,|\hat{Q}_{l_a}^m\,|LM'_L\rangle\,\langle\Lambda\,|q_{l_b}^{m'}\,|\Lambda'\rangle\,\delta_{M_a,m}\delta_{M_b,m'} \tag{10}$$

and $n = l_a + l_b + 1$. To simplify the notation, $i$ stands for $\{LM_L\}$ and $i'$ for $\{L'M'_L\}$ for carbon , $j = \{\Lambda\}$ and $j' = \{\Lambda'\}$ for OH. In present work, we have considered the electrostatic energies of Eq. 9 including the dipole-quadrupole ($l_a = 2, l_b = 1$) and quadrupole-quadrupole ($l_a = l_b = 2$) interactions. In such a case, the permanent dipole and quadrupole moments of OH as well as the permanent quadrupole moment of carbon atom are required to evaluate the interaction coefficients of Eq. 10.

### B. Formalism for the dispersion energy

From second-order perturbation theory, the dispersion energy results from induced-multipole induced-multipole interactions and can be written as

$$E_{\rm disp}^{JM_JJ'M'_J\Lambda\Sigma\Lambda'\Sigma'} = -\sum_{l_al_bl'_al'_b}\frac{1}{R^n}\sum_{M_LM_SM'_LM'_S}\langle LSM_LM_S \mid JM_J\rangle\langle LSM'_LM'_S \mid J'M'_J\rangle\,\delta_{M_SM'_S}\delta_{\Sigma\Sigma'}$$
$$\times\sum_{m=-l_<}^{l_<} g_m(l_a,l_b)\sum_{m'=-l'_<}^{l'_<} g_{m'}(l'_a,l'_b)\sum_{k_bk'_b} d^{l_b}_{-mk_b}(\gamma)d^{l'_b}_{-m'k'_b}(\gamma) \qquad (11)$$
$$\times\sum_{\Gamma''_a\Gamma''_b}\frac{\langle LM_L\,|\hat{Q}^m_{l_a}\,|L''M''_L\rangle\langle L''M''_L\,|\hat{Q}^{m'}_{l'_a}\,|L'M'_L\rangle\langle\Lambda\,|\hat{q}^{k_b}_{l_b}\,|\Lambda''\rangle\langle\Lambda''\,|\hat{q}^{k'_b}_{l'_b}\,|\Lambda'\rangle}{\epsilon''_a+\epsilon''_b}$$

where $n = l_a + l'_a + l_b + l'_b + 2$ and $\epsilon'' = E_{\Gamma''} - E_0$ is the energy difference between the ground and excited-states labelled $\Gamma'' = \{\gamma'' L'' M''_L\}$ or $\{\gamma''\Lambda''\}$, where $\gamma''$ stands for all other quantum numbers necessary to define the monomer state.

Using the following definition for the imaginary frequency-dependent polarizabilities associated with each monomer

$${}^{ii'}\alpha_{lml'm'}(i\omega) = \sum_{\Psi''}\frac{2\epsilon''\langle\Psi^i_0\,|\hat{Q}^m_l\,|\Psi''\rangle\langle\Psi''\,|\hat{Q}^{m'}_{l'}\,|\Psi^{i'}_0\rangle}{\epsilon''^2+\omega^2} \qquad (12)$$

where $i, i'$ stand for $\{LM_L\}, \{L'M'_L\}$ for carbon or $\{\Lambda\}, \{\Lambda'\}$ for OH, and using the Casimir-Polder integral transformation, one has

$$D^{ii'jj'}_{l_al'_aml_bl'_bk_b} = \sum_{\Gamma''_a\Gamma''_b}\frac{\langle LM_L\,|\hat{Q}^m_{l_a}\,|L''M''_L\rangle\langle L''M''_L\,|\hat{Q}^{m'}_{l'_a}\,|L'M'_L\rangle\langle\Lambda\,|\hat{q}^{k_b}_{l_b}\,|\Lambda''\rangle\langle\Lambda''\,|\hat{q}^{k'_b}_{l'_b}\,|\Lambda'\rangle}{\epsilon''_a+\epsilon''_b}$$
$$= \frac{1}{2\pi}\int_0^\infty d\omega\;{}^{ii'}\alpha_{l_aml'_am'}(i\omega)\;{}^{jj'}\alpha_{l_bk_bl'_bk'_b}(i\omega). \qquad (13)$$

The integrals $D^{ii'jj'}_{l_al'_aml_bl'_bk_b}$ are zero unless $m' = M_L - M'_L - m$ and $k'_b = \Lambda - \Lambda' - k_b$, so that the quantum numbers $m'$ and $k'_b$ have been omitted in the label of these quantities. Following Spelsberg et al. [18], coupled quantities can either be defined as

$$D^{ii'jj'}_{(l_al'_a)L_aM_a(l_bl'_b)L_bM_b} = \sum_{mm'k_bk'_b}\langle l_aml'_am'\mid L_aM_a\rangle\langle l_bk_bl'_bk'_b\mid L_bM_b\rangle\,D^{ii'jj'}_{l_al'_aml_bl'_bk_b}$$
$$= \frac{1}{2\pi}\int_0^\infty d\omega\;{}^{ii'}\alpha_{(l_al'_a)L_aM_a}(i\omega)\;{}^{jj'}\alpha_{(l_bl'_b)L_bM_b} \qquad (14)$$

where the coupled dynamic polarizabilities are defined as

$$ {}^{ii'}\alpha_{(ll')LM}(i\omega) = \sum_{mm'} \langle lml'm' \mid LM \rangle \ {}^{ii'}\alpha_{lml'm'}(i\omega). \tag{15} $$

From the Clebsch-Gordan coefficients of Eqs. 14 and 15, it follows that the coupled Casimir-Polder integrals are zero unless $M_a = m+m' = M_L - M'_L$ for carbon and $M_b = k_b + k'_b = \Lambda - \Lambda'$ for OH. Furthermore, we use the following contraction scheme

$$ d^{l_b}_{-mk_b}(\gamma) d^{l'_b}_{-m'k'_b}(\gamma) = \sum_{L_b M M_b} \langle l_b k_b l'_b k'_b \mid LM_b \rangle \langle l_b - m l'_b - m' \mid L - M \rangle \, d^{L_b}_{-MM_b}(\gamma). \tag{16} $$

from which it follows that $M = m + m' = M_a$ from above.

Using Rels. 11,13, 14 and 16, the final expression for the dispersion energy matrix elements in the $|JM_J\rangle \, |\Lambda, \Sigma\rangle$ diabatic basis set writes

$$ \begin{aligned} E^{JM_J J' M'_J \Lambda \Sigma \Lambda' \Sigma'}_{\rm disp} &= -\sum_{l_a l_b l'_a l'_b} \frac{1}{R^n} \sum_{M_L M_S M'_L M'_S} \langle LSM_L M_S \mid JM_J \rangle \langle LSM'_L M'_S \mid J' M'_J \rangle \, \delta_{M_S M'_S} \delta_{\Sigma\Sigma'} \\ &\times \sum_{L_a L_b M_a M_b} g_2(l_a, l'_a, l_b, l'_b, L_a, L_b, M_a) D^{ii'jj'}_{(l_a l'_a) L_a M_a (l_b l'_b) L_b M_b} d^{L_b}_{-M_a M_b}(\gamma) \end{aligned} \tag{17} $$

where $n = l_a + l'_a + l_b + l'_b + 2$ and the $g_2$ coefficient (defined by Rel.(10) of Ref. [10]) reads

$$ \begin{aligned} & g_2(l_a, l'_a, l_b, l'_b, L_a, L_b, M_a) = \sum_{mm'\lambda} g_m(l_a, l_b) g_{m'}(l'_a, l'_b) \langle l_b - m l'_b - m' \mid L_b - M_a \rangle \langle l_a m l'_a m' \mid L_a M_a \rangle \\ &= (-1)^{l_b + l'_b} \left[ \begin{pmatrix} 2L_{ab} \\ 2l_a \end{pmatrix} \begin{pmatrix} 2L'_{ab} \\ 2l'_a \end{pmatrix} \right]^{1/2} \left[ (2L_{ab}+1)(2L'_{ab}+1)(2L_a+1)(2L_b+1) \right]^{1/2} \\ &\times \langle L_{ab} 0 L'_{ab} 0 \mid \lambda 0 \rangle \langle L_a M_a L_b - M_a \mid \lambda 0 \rangle \begin{Bmatrix} l_a & l'_a & L_a \\ l_b & l'_b & L_b \\ L_{ab} & L'_{ab} & \lambda \end{Bmatrix} \delta_{L_{ab}, l_a + l_b} \delta_{L'_{ab}, l'_a + l'_b} \end{aligned} \tag{18} $$

The dispersion energy matrix elements can also be expanded as

$$ \begin{aligned} E^{JM_J J' M'_J \Lambda \Sigma \Lambda' \Sigma'}_{\rm disp} &= -\sum_{l_a l_b l'_a l'_b} \frac{1}{R^n} \sum_{M_L M_S M'_L M'_S} \langle LSM_L M_S \mid JM_J \rangle \langle LSM'_L M'_S \mid J' M'_J \rangle \\ &\times \delta_{M_S M'_S} \delta_{\Sigma\Sigma'} \sum_{L_b M_a M_b} {}^{ii'jj'}V^{\rm disp}_{nL_b M_a M_b} \, d^{L_b}_{-M_a M_b}(\gamma) \end{aligned} \tag{19} $$

where the dispersion interaction coefficients ${}^{ii'jj'}V^{\rm disp}_{nL_b M_a M_b}$ write

$$ {}^{ii'jj'}V^{\rm disp}_{nL_b M_a M_b} = \sum_{L_a} g_2(l_a, l'_a, l_b, l'_b, L_a, L_b, M_a) D^{ii'jj'}_{(l_a l'_a) L_a M_a (l_b l'_b) L_b M_b} \tag{20} $$

and are zero unless $M_a = M_L - M'_L$ and $M_b = \Lambda - \Lambda'$. In present work, we have considered the dipole-induced dipole-induced interactions ($l_a = l_b = l'_a = l'_b = 1$) and truncated the expansion of Eq. 19 after terms in $R^{-6}$. In such a case, the dipole dynamic polarizabilities of C and OH are needed to evaluate the interaction coefficients of Eq. 20.

### C. Formalism for the induction energy

If one of the two monomers has a permanent multipole, second-order perturbation theory leads to the induction energy, which results from the interaction between a permanent multipole and an induced-multipole. It can be written as

$$\begin{aligned} E_{\rm ind}^{JM_JJ'M'_J\Lambda\Sigma\Lambda'\Sigma'} &= -\sum_{l_al_bl'_al'_b} \frac{1}{R^n} \sum_{M_LM_SM'_LM'_S} \langle LSM_LM_S \mid JM_J\rangle \langle LSM'_LM'_S \mid J'M'_J\rangle \, \delta_{M_SM'_S}\delta_{\Sigma\Sigma'} \\ &\times \sum_{m=-l_<}^{l_<} g_m(l_a,l_b) \sum_{m'=-l'_<}^{l'_<} g_{m'}(l'_a,l'_b) \sum_{k_bk'_b} d^{l_b}_{-mk_b}(\gamma) d^{l'_b}_{-m'k'_b}(\gamma) \\ &\times \sum_{\Gamma''_a} \frac{\langle LM_L \,|\hat{Q}^m_{l_a}\,| L''M''_L\rangle \langle L''M''_L \,|\hat{Q}^{m'}_{l'_a}\,| L'M'_L\rangle}{\epsilon''_a} \langle \Lambda \,|\hat{q}^{k_b}_{l_b}\,|\Lambda'\rangle \langle \Lambda' \,|\hat{q}^{k'_b}_{l'_b}\,|\Lambda\rangle \end{aligned} \tag{21}$$

where, again, $n = l_a + l'_a + l_b + l'_b + 2$. The Wigner-Eckart theorem implies that $k_b = -k'_b = \Lambda - \Lambda' = 0, \pm 2$ (for a $\Pi$ state diatom).

Using the following definition for the atomic static polarizability

$${}^{LM_LLM'_L}\alpha_{lml'm'} = 2\sum_{\Gamma''} \frac{\langle LM_L \,|\hat{Q}^m_l\,| L''M''_L\rangle \langle L''M''_L \,|\hat{Q}^{m'}_{l'}\,| LM'_L\rangle}{\epsilon''} \tag{22}$$

and using the contraction scheme given by Eq. 16, then Eq. 21 reads

$$\begin{aligned} E_{\rm ind}^{JM_JJ'M'_J\Lambda\Sigma\Lambda'\Sigma'} &= -\sum_{l_al_bl'_al'_b} \frac{1}{R^n} \sum_{M_LM_SM'_LM'_S} \langle LSM_LM_S \mid JM_J\rangle \langle LSM'_LM'_S \mid J'M'_J\rangle \\ &\times \delta_{M_SM'_S}\delta_{\Sigma\Sigma'} \sum_{L_b}{}^{ii'jj'}V^{\rm ind}_{nL_bM_a0}\; d^{L_b}_{-M_a0}(\gamma) \end{aligned} \tag{23}$$

where the induction interaction coefficients ${}^{ii'jj'}V^{\rm ind}_{nL_bM_a0}$ read

$$
\begin{aligned}
{}^{ii'jj'}V^{\rm ind}_{nL_bM_a0} \;=\; & \sum_{m=-l_<}^{l_<} g_m(l_a,l_b) \sum_{m'=-l'_<}^{l'_<} g_{m'}(l'_a,l'_b) \\
& \times \langle l_b(\Lambda-\Lambda')l'_b(\Lambda'-\Lambda) \mid L_b 0\rangle \;\; \langle l_b - m l'_b - m' \mid L_b - M_a\rangle \\
& \times \langle \Lambda \mid \hat{q}_{l_b}^{(\Lambda-\Lambda')} \mid \Lambda'\rangle \, \langle \Lambda' \mid \hat{q}_{l'_b}^{(\Lambda'-\Lambda)} \mid \Lambda'\rangle \, \frac{{}^{ii'}\alpha_{l_a m l'_a m'}}{2}
\end{aligned}
\tag{24}
$$

where $< \Lambda|\hat{q}_{l_b}^{k_b}|\Lambda' >$ are the permanent multipole moments of monomer B (i.e. OH). Again, matrix elements of Eq. 24 are zero unless $M_a = m+m' = M_L - M'_L$. We have considered here the dipole dipole-induced contribution ($l_a = l_b = l'_a = l'_b = 1$) and truncated the expansion of Eq. 23 after terms in $R^{-6}$. The permanent dipole moment of OH and the static dipole polarizabilities of carbon atom are thus required to determine the interaction coefficients of Eq. 24.

## III. RESULTS AND DISCUSSION

### A. Permanent multipole moments

We present in Table I values for the permanent dipole and quadrupole moments of C($^3P$) and OH($X^2\Pi$) which have been employed in the present work to derive the C+OH interaction coefficients. For OH, we have taken the experimental value of Ref. [19] for $Q_1^0$, and the most recent *ab initio* values of Ref. [9] for $Q_2^0$ and $Q_2^{\pm 2}$, corresponding to MRCI calculations with aug-cc-pVTZ basis set. For C($^3P$), we have taken the $Q_2^0$ experimental value of Ref. [23].

### B. Static and dynamic polarizabilities

To evaluate properly the polarization energy (induction plus dispersion contributions), accurate values of the static (for carbon atom only) and dynamic polarizabilities (for C and OH) are required. For OH, we have generated the dynamic polarizabilities from the pseudo-oscillator strengths and pseudo-energies tabulated by Spelsberg in Ref. [10] for ${}^{xx}\alpha^{\pm\pm}_{lml'm'}$ and ${}^{xy}\alpha^{\pm\mp}_{lml'm'}$. Those values were computed by means of single-excitation MRCI calculations (SE-MRCI) within the averaged coupled pair functional formalism (ACPF) and the basis set of Ref. [25]. It is worth to note that the polarizabilities of Ref. [10] correspond to electronic

wavefunctions and multipole moment operators of definite symmetry with respect to $\sigma_{xz}$, the reflection through the $xz$ plane. In such a case, the symmetrized wavefunctions are labeled $|(\Lambda=1)^+\rangle = |\Pi^+\rangle = |x\rangle$ and $|(\Lambda=1)^-\rangle = |\Pi^-\rangle = |y\rangle$. We have also the following equivalences between the present notation for cartesian polarisabilities and those given in Ref. [10]: ${}^{xx}\alpha_{zz} = {}^{xx}\ \alpha^{++}_{1010}(\ [10])$, ${}^{xx}\alpha_{xx} = {}^{xx}\ \alpha^{++}_{1111}(\ [10])$, and ${}^{xx}\alpha_{yy} = {}^{xx}\ \alpha^{--}_{1111}(\ [10])$ for the $|x\rangle$ state (and equivalently for the $|y\rangle$ state). The latter cartesian components are reported in Table II together with literature values. The corresponding dynamic components are also tabulated in Table II at selected values of the imaginary frequency. Furthermore, while *ab initio* calculations furnish cartesian components of the polarizabilities, the associated spherical components are required to determine the interaction coefficients given by Eq. 20. Relations between both components are given in Appendix C and result from the inversion of Rel.(19) of Ref. [10]

$$\hat{Q}^m_l = \sqrt{\frac{(1+\delta_{m0})}{2}}(-\sigma_m)^m[\hat{Q}^+_{l|m|} + i\sigma_m\hat{Q}^-_{l|m|}] \tag{25}$$

where $\sigma_m$=sign($m$) and $\pm$ is the parity by reflection through the $xz$ plane. An equivalent relation is used to relate the complex wavefunctions $|\Lambda=\pm1\rangle$ to the real ones $|(\Lambda=1)^\pm\rangle$ of definite symmetry.

For carbon, the dynamic polarizabilities have been calculated by means of the MCSCF linear response method [27] as implemented in *ab initio* quantum chemistry code of Dalton [28]. We performed CASSCF calculations including 13 orbitals $(2s, 2p, 3s, 3p, 3d)$ and 4 electrons in the active space with the aug-cc-pVQZ basis set, which provided a set of Cauchy moments for each of the $M_L$ substate. Then we used analytical continuation techniques following the $[n, n-1]_\alpha$ and $[n, n-1]_\beta$ Padé approximants procedures defined in Ref. [29] to get lower and upper bounds to the dynamic polarizabilities ${}^{LM_L}\alpha_{zz}(i\omega)$. With $n=10$, the associated dispersion coefficients $C_6^{\mathrm{C-C}}$ are found to be converged within 0.02%. Parallel ${}^{LM_L}\alpha_{zz}$ and perpendicular ${}^{LM_L}\alpha_{xx}$ components of the static polarisability associated with the $M_L=0$ substate are reported in Table II together with literature values (for atoms in a $P$ state ${}^{LM_L=\pm1}\alpha_{zz} = {}^{LM_L=0}\alpha_{xx}$). The corresponding dynamic components are also tabulated in Table II at selected values of the imaginary frequency. To get the whole set of spherical components of polarizability needed in Eqs. 20 and 24, we followed Chu et al. [30] and derived an extention of Eq.(A5) of Ref. [30] including diagonal ($M_L = M'_L$) and

off-diagonal ($M_L \neq M'_L$) spherical components of polarizability:

$$^{LM_L LM'_L}\alpha_{lml'm'}(i\omega) = \sum_{KQ} {}^{L}\alpha_{(ll')K}(i\omega)(-1)^{M_L+M'_L} \frac{\langle lml'm' \mid KQ\rangle \langle LM_L K-Q \mid LM'_L\rangle}{\langle l0l'0 \mid K0\rangle \langle LLK0 \mid LL\rangle} \quad (26)$$

where the reduced matrix element ${}^{L}\alpha_{(ll')K}(i\omega)$ is defined as

$$\begin{aligned} {}^{L}\alpha_{(ll')K}(i\omega) \;=\; & \frac{\sqrt{(2K+1)}}{\sqrt{(2L+1)}} \sum_{\Gamma''} \frac{2\epsilon'' \langle L \mid\mid \hat{Q}_l \mid\mid L''\rangle \langle L'' \mid\mid \hat{Q}_{l'} \mid\mid L\rangle}{\epsilon''^2+\omega^2} \begin{Bmatrix} LL''l \\ l'KL \end{Bmatrix} \\ & \times \langle l0l'0 \mid K0\rangle \langle LLK0 \mid LL\rangle \end{aligned} \quad (27)$$

In the case of dipole polarizabilities, $l = l'$=1. For symmetry reason, in present case, only ${}^{L}\alpha_{(ll')K}(i\omega)$ with even $K$ will contribute to the C+OH interaction coefficients, so that the knowledge of ${}^{L}\alpha_{(11)0}$ and ${}^{L}\alpha_{(11)2}$ is suffisant to get the whole set of $^{LM_L LM'_L}\alpha_{lml'm'}$ spherical components. These two quantities were derived from the calculated diagonal components $^{LM_L LM_L}\alpha_{1010}(i\omega) = {}^{LM_L}\alpha_{zz}(i\omega)$ using the relation

$$^{LM_L LM_L}\alpha_{1010}(i\omega) \;=\; {}^{L}\alpha_{(11)0}(i\omega) + {}^{L}\alpha_{(11)2}(i\omega) \frac{\langle LM_L 20 \mid LM_L\rangle}{\langle LL20 \mid LL\rangle} \quad (28)$$

$$\;=\; {}^{L}\alpha_{(11)0}(i\omega) + {}^{L}\alpha_{(11)2}(i\omega) \frac{3M_L^2 - L(L+1)}{L(2L-1)} \quad (29)$$

from which we obtain the inverse relations for $M_L$=0 and $M_L = \pm 1$

$${}^{L}\alpha_{(11)0}(i\omega) \;=\; \frac{2\,{}^{LM_L=\pm1}\alpha_{zz}(i\omega) + {}^{LM_L=0}\alpha_{zz}(i\omega)}{3} \quad (30)$$

$${}^{L}\alpha_{(11)2}(i\omega) \;=\; \frac{{}^{LM_L=\pm1}\alpha_{zz}(i\omega) - {}^{LM_L=0}\alpha_{zz}(i\omega)}{3} \quad (31)$$

### C. Interaction coefficients

From the knowledge of permanent multipole, static and dynamic polarisabilities of C($^3P$) and OH($X^2\Pi$), long range multipolar matrix elements $^{ii'jj'}V_{nL_bM_aM_b}$ can be evaluated for the electrostatic (Eq. 10), induction (Eq. 24) and dispersion (Eq. 20) energies. The $^{ii'jj'}V_{nL_bM_aM_b}$ coefficients are given in $LS$ coupling case in Tables III and IV for the electrostatic and polarization (induction plus dispersion) contributions, respectively, where $i$ or $i'$ stands for $|LSM_LM_S\rangle$ for C($^3P$) (with $L = S = 1$) and $j$ or $j'$ stands for $|\Lambda\Sigma\rangle$ for OH($X^2\Pi$) (with $\Lambda = \pm 1$, $\Sigma = \pm\frac{1}{2}$). Rels. 9, 19 and 23 will then generate the related coefficients in $JJ$ coupling case, i.e. in the $|JM_J\rangle$ basis for carbon and in the doubly degenerate $|\pm\Omega\rangle$ basis

for OH. In this last case, the $|\pm\Omega\rangle$ set of wavefunctions are directly obtained from those in the $LS$ coupling case by the relations $|\pm\Omega\rangle = |\pm\Lambda\pm\Sigma\rangle$ or $|\pm\Omega\rangle = |\pm\Lambda\mp\Sigma\rangle$.

In present work, the electrostatic coefficients have been tabulated for the dipole-quadrupole (n=4) and quadrupole-quadrupole (n=5) interactions, the dispersion coefficients for the dipole-induced dipole-induced (n=6) interactions and the induction coefficients for dipole dipole-induced interaction (n=6). Notice that the induction coefficients vanish for off-diagonal matrix elements $|\Lambda - \Lambda'| = 2$, due to the restriction given by $|\Lambda - \Lambda'| \leq l_b$, where $l_b$=1 for dipole. To the best of our knowledge, the C-OH interaction coefficients are determined here for the first time, and thus, there is no possible comparison with other tabulated values. Nevertheless, estimated values of state-averaged coefficients for dispersion and induction contributions can be retrieved following Nielson et al. [31] i.e. for $C_6$(0,ind) (Eq. 32b), $C_6$(0,disp) (Eq. 41) and $C_6$(2,disp) (Eq.42). Using the dipole moment and static polarizabilities values of Tables I and II, together with the rough London approximation to evaluate the dispersion coefficients as was used in Ref. [23], we get $C_6$(0,ind)=-4.955 a.u., $C_6$(0,disp)=-31.89 a.u. and $C_6$(2,disp)=-2.52 a.u. These values are found in good agreement with present state-averaged coefficients i.e. -4.955, -35.93, -2.73 a.u. respectively.

### D. Long-range multipolar potentials

The full multipolar potential has been determined in the $|JM_J\rangle|\Lambda\Sigma\rangle$ basis set from

$$E_{\rm tot}^{JM_JJ'M'_J\Lambda\Sigma\Lambda'\Sigma'} = E_{\rm elec}^{JM_JJ'M'_J\Lambda\Sigma\Lambda'\Sigma'} + E_{\rm disp}^{JM_JJ'M'_J\Lambda\Sigma\Lambda'\Sigma'} + E_{\rm ind}^{JM_JJ'M'_J\Lambda\Sigma\Lambda'\Sigma'} + E_{\rm SO}^{JM_JJ'M'_J\Lambda\Sigma\Lambda'\Sigma'} \tag{32}$$

where the electrostatic, dispersion and induction contribution are given by Eqs. 9, 19 and 23, respectively. The spin-orbit contribution $E_{\rm SO}^{JM_JJ'M'_J\Lambda\Sigma\Lambda'\Sigma'}$ vanish unless $J' = J, M'_J = M_J, \Lambda' = \Lambda$ and $\Sigma' = \Sigma$, and the non-zero diagonal matrix elements write as a function of the fine structure splittings $\delta_{\rm OH}$ and $\delta_{J,\rm C}$. By sorting the $|JM_J\rangle$ states in the order C($^3P_2$), C($^3P_1$) and C($^3P_0$) with $M_J$ indices running from top to bottom as $M_J = J$ to $M_J = -J$, the 18 spin-orbit matrix elements write as follows: $\{\delta_{2,\rm C}+\delta_{\rm OH},\ \delta_{2,\rm C}+\delta_{\rm OH},\ \delta_{2,\rm C}+\delta_{\rm OH},\ \delta_{2,\rm C}+\delta_{\rm OH},\ \delta_{2,\rm C}+\delta_{\rm OH},\ \delta_{1,\rm C}+\delta_{\rm OH},\ \delta_{1,\rm C}+\delta_{\rm OH},\ \delta_{1,\rm C}+\delta_{\rm OH},\ \delta_{\rm OH}\}$ for the first 9 states $|JM_J\rangle|\Lambda\Sigma\rangle$, and $\{\delta_{2,\rm C},\ \delta_{2,\rm C},\ \delta_{2,\rm C},\ \delta_{2,\rm C},\ \delta_{2,\rm C},\ \delta_{1,\rm C},\ \delta_{1,\rm C},\ \delta_{1,\rm C},\ 0\}$ for the remaining 9 states. The upper 9 states correspond to $|\Lambda = \pm1, \Sigma = \mp1/2\rangle$ while the lower 9 states correspond to $|\Lambda = \pm1, \Sigma = \pm1/2\rangle$. The fine structure splitting values have been taken equal to the

experimental values $\delta_{\rm OH} = 139.7$ cm$^{-1}$ [33], $\delta_{1,\rm C} = 16.4$ cm$^{-1}$ and $\delta_{2,\rm C} = 43.4$ cm$^{-1}$ [34]. Using the tabulated values for the $V^{ii'jj'}_{nL_bM_aM_b}$ matrix elements, the full multipolar potential matrix has been computed from Eq. 32, and subsequently diagonalized to compare the resulting adiabatic long range multipolar PESs with *ab initio* PESs provided by supermolecular calculations.

We compare in Figs. 1 and 2 the pure multipolar long-range potentials including electrostatic and induction contributions only with *ab initio* potentials evaluated at the CASSCF level [7] for the 12 non-relativistic states of C+OH, i.e. neglecting the spin-orbit interaction. The potentials are plotted as a function of the intermolecular distance $R$ for $\gamma = 0°$ in Fig. 1a and for $\gamma = 180°$ in Fig. 1b, as well as a function of $\gamma$ for $R = 25$ bohr in Fig. 2. When spin-orbit interactions are neglected, the $^{2,4}\Sigma^+$,$^{2,4}\,\Delta$,$^{2,4}\,\Sigma^-$ states form one group of quasi-degenerate states with an attractive behavior at $\gamma = 0°$ and with a repulsive behavior at $\gamma = 180°$,while the $^{2,4}\Pi$ states display opposite behavior. As can be seen in Figs. 1 and 2 for the doublet states (degenerate with their quartet counterparts at long-range), the multipolar and *ab initio* interaction potentials display a similar behavior and are found in a quantitative quite good agreement. The remaining small differences may result from the use of different basis sets in the two calculations and from the uncorrected basis set superposition errors (BSSE) of the CASSCF energies.

Full multipolar potentials including spin-orbit splitting have been plotted for the 18 spin-orbit states of C+OH as a function of the intermolecular distance $R$ for $\gamma = 0°$ in Fig. 3a and for $\gamma = 180°$ in Fig. 3b, as well as a function of $\gamma$ at $R = 10$ bohr in Fig. 4. In these figures, the states are labelled according to the value of the quantum number $\Omega = M_J + \Lambda + \Sigma$, well defined for linear geometries of the complex. At short distance, once the spin-orbit splitting becomes smaller than the binding energies, these states correlate to the $^{2S+1}\Lambda$ states and converge towards two groups of states as previously observed in Fig. 1. Nevertheless, due to the contribution of dispersion energies, the group of states which displayed a repulsive behavior for $\gamma = 180°$ in Fig. 1b becomes attractive at short distance and small potential barriers are observed around 7-8 bohr. In Fig. 4, we observe a quasi-isotropic potential for the C+OH ground state. A slight preference appears for the approach of the carbon atom on the hydrogen side of OH while the oxygen side is preferred in Fig 2 when spin-orbit splittings are neglected. The complex spin-orbit structure of the long-range states of C + OH shows also some conical intersections between states with same $\Omega$ value, as can be seen

in the 100-130 $cm^{-1}$ energy range of Fig. 3a ($\gamma = 0°$) or in the -50-40 $cm^{-1}$ energy range of Fig. 3b ($\gamma = 180°$).

## IV. CONCLUSION

We have calculated the long-range intermolecular potentials of the 18 spin-orbit states resulting from the interaction between the two open-shell systems C($^3$P) and OH($X^2\Pi$). The diatomic OH has been kept fixed at its ground vibrational state averaged distance $r_0$. The long-range interaction potentials are thus two-dimensional potential energy surfaces (PESs) that depend on the intermolecular distance $R$ and the angle $\gamma$ between $\mathbf{R}$ and $\mathbf{r}$. The potential matrix elements have been evaluated within a diabatic basis set, built over the unperturbed electronic wavefunctions of C and OH, and from the perturbation theory up to second order using a two-center expansion of the coulombic intermolecular potential operator. This gives rise to a multipolar expansion of the potential expressed as a series of terms varying in $R^{-n}$. The formalism to evaluate the long-range coefficients of such an expansion is explicitly given for the first-order electrostatic and second-order polarization (dispersion plus induction) contributions. The electrostatic energies include the dipole-quadrupole (in $R^{-4}$) and quadrupole-quadrupole (in $R^{-5}$) interactions, while the dispersion and induction energies have been limited to the terms varying in $R^{-6}$, i.e. terms that include the dipole-induced dipole-induced (dispersion) and dipole dipole-induced (induction) interactions. The determination of the coefficients relies on the knowledge of monomer properties such as the permanent multipole moments, static and dynamic polarizabilities which have been carrefully calculated or selected from literature values. The final potential matrix incorporates the atomic and diatomic spin-orbit splittings. The diagonalization of the 18 $\times$ 18 full potential matrix generates the adiabatic long-range PESs. A comparison of the present potentials with their *ab initio* counterparts obtained at the CASSCF level within a supermolecule formalism has been undergoing, and a good agreement between both approaches is observed.

**ACKNOWLEDGMENTS**

BBH acknowledges support from the "Institut du Développement des Ressources en Informatique Scientifique" (IDRIS) in Orsay (France) and from UTINAM computer center.

**APPENDIX A**

In this appendix, explicit expressions of the $\langle JM_J \,|\hat{Q}_2^m\,|J'M'_J\rangle$ quadrupole matrix elements of carbon are given. Following the work of Graff and Wagner [8] and of Gentry and Giese [17], we have expressed the $9 \times 9$ matrices as a function of the $Q_2(\mathrm{C}) = 2\,\langle L0\,|\hat{Q}_2^0\,|L0\rangle$ quantity (noted $Q_0$ in Ref. [8]). From the relation,

$$\langle JM_J\,|\hat{Q}_{l_a}^m\,|J'M'_J\rangle \;=\; (-1)^{J'-M_J+l_a}\sqrt{(2J+1)(2J'+1)}\begin{pmatrix} J' & J & l_a \\ M' & -M & M-M' \end{pmatrix}\begin{Bmatrix} L & L & l_a \\ J' & J & S \end{Bmatrix} \times \langle L\,||\hat{Q}_{l_a}\,||L\rangle \tag{33}$$

and with the following definition

$$Q_2(\mathrm{C}) = 2\,\langle L0\,|\hat{Q}_2^0\,|L0\rangle = 2(-1)^L\begin{pmatrix} L & 2 & L \\ 0 & 0 & 0 \end{pmatrix}\langle L|\,|\hat{Q}_2\,||L\rangle\,, \tag{34}$$

we obtain

$$
\begin{array}{rccccccccc}
State: & & & {}^3P_2 & & & & {}^3P_1 & & {}^3P_0 \\
M_J: & 2 & 1 & 0 & -1 & -2 & 1 & 0 & -1 & 0
\end{array}
$$

$$
\left\langle \hat{Q}_2^0(\mathrm{C}) \right\rangle = \frac{Q_2(\mathrm{C})}{4}
\begin{pmatrix}
-1 & 0 & 0 & 0 & 0 & 0 & 0 & 0 & 0 \\
0 & 1/2 & 0 & 0 & 0 & -3/2 & 0 & 0 & 0 \\
0 & 0 & 1 & 0 & 0 & 0 & 0 & 0 & -\sqrt{2} \\
0 & 0 & 0 & 1/2 & 0 & 0 & 0 & 3/2 & 0 \\
0 & 0 & 0 & 0 & -1 & 0 & 0 & 0 & 0 \\
0 & -3/2 & 0 & 0 & 0 & 1/2 & 0 & 0 & 0 \\
0 & 0 & 0 & 0 & 0 & 0 & -1 & 0 & 0 \\
0 & 0 & 0 & 3/2 & 0 & 0 & 0 & 1/2 & 0 \\
0 & 0 & -\sqrt{2} & 0 & 0 & 0 & 0 & 0 & 0
\end{pmatrix}, \qquad (35)
$$

$$
\begin{array}{rccccccccc}
State: & & & {}^3P_2 & & & & {}^3P_1 & & {}^3P_0 \\
M_J: & 2 & 1 & 0 & -1 & -2 & 1 & 0 & -1 & 0
\end{array}
$$

$$
\left\langle \hat{Q}_2^1(\mathrm{C}) \right\rangle = \frac{3Q_2(\mathrm{C})}{2\sqrt{2}}
\begin{pmatrix}
0 & 1/\sqrt{2} & 0 & 0 & 0 & -1/\sqrt{2} & 0 & 0 & 0 \\
0 & 0 & 1/\sqrt{12} & 0 & 0 & 0 & 1/2 & 0 & -\sqrt{2/3} \\
0 & 0 & 0 & -1/\sqrt{12} & 0 & 0 & 0 & \sqrt{3/4} & 0 \\
0 & 0 & 0 & 0 & -1/\sqrt{2} & 0 & 0 & 0 & 0 \\
0 & 0 & 0 & 0 & 0 & 0 & 0 & 0 & 0 \\
0 & 0 & \sqrt{3/4} & 0 & 0 & 0 & -1/2 & 0 & 0 \\
0 & 0 & 0 & 1/2 & 0 & 0 & 0 & 1/2 & 0 \\
0 & 0 & 0 & 0 & -1/\sqrt{2} & 0 & 0 & 0 & 0 \\
0 & 0 & 0 & \sqrt{2/3} & 0 & 0 & 0 & 0 & 0
\end{pmatrix}, \qquad (36)
$$

$$
\begin{array}{rccccccccc}
State: & & & {}^3P_2 & & & & {}^3P_1 & & {}^3P_0 \\
M_J: & 2 & 1 & 0 & -1 & -2 & 1 & 0 & -1 & 0
\end{array}
$$

$$
\left\langle \hat{Q}_2^2(\mathrm{C}) \right\rangle = 3Q_2(\mathrm{C}) \begin{pmatrix}
0 & 0 & -1/\sqrt{6} & 0 & 0 & 0 & 1/\sqrt{2} & 0 & -1/\sqrt{3} \\
0 & 0 & 0 & -1/2 & 0 & 0 & 0 & 1/2 & 0 \\
0 & 0 & 0 & 0 & -1/\sqrt{6} & 0 & 0 & 0 & 0 \\
0 & 0 & 0 & 0 & 0 & 0 & 0 & 0 & 0 \\
0 & 0 & 0 & 0 & 0 & 0 & 0 & 0 & 0 \\
0 & 0 & 0 & -1/2 & 0 & 0 & 0 & 1/2 & 0 \\
0 & 0 & 0 & 0 & -1/\sqrt{2} & 0 & 0 & 0 & 0 \\
0 & 0 & 0 & 0 & 0 & 0 & 0 & 0 & 0 \\
0 & 0 & 0 & 0 & -1/\sqrt{3} & 0 & 0 & 0 & 0
\end{pmatrix} \tag{37}
$$

## V. APPENDIX B

In this appendix, we give the explicit $\gamma$-dependence of the reduced $d^l_{mm'}$ rotation matrices used in this work:

| l | m | m' | $d^l_{mm'}$ | l | m | m' | $d^l_{mm'}$ |
|---|---|---|---|---|---|---|---|
| 1 | 0 | 0 | $\cos(\gamma)$ | 2 | 2 | 0 | $\frac{\sqrt{6}}{4}\sin^2(\gamma)$ |
| 1 | 1 | 0 | $-\frac{\sin(\gamma)}{\sqrt{2}}$ | 2 | 2 | 1 | $-\frac{1+\cos(\gamma)}{2}\sin(\gamma)$ |
| 2 | 0 | 0 | $\frac{3}{2}\cos^2(\gamma)-\frac{1}{2}$ | 2 | 2 | -1 | $-\frac{1-\cos(\gamma)}{2}\sin(\gamma)$ |
| 2 | 1 | 0 | $-\sqrt{\frac{3}{2}}\sin(\gamma)\cos(\gamma)$ | 2 | 2 | 2 | $[\frac{1+\cos(\gamma)}{2}]^2$ |
| | | | | 2 | 2 | -2 | $[\frac{1-\cos(\gamma)}{2}]^2$ |

Usual relations[32] hold to get other rotation matrices,

$$d^l_{mm'} = d^l_{-m'-m} = (-1)^{m'-m} d^l_{m'm}$$

## VI. APPENDIX C

Using the following definition for the spherical components of the dynamic polarizability of OH in the $|\Lambda = \pm 1\rangle$ electronic basis set

$$ {}^{\Lambda\Lambda'}\alpha_{lml'm'}(i\omega) = \sum_{\Gamma''} \frac{2\epsilon'' \langle \Lambda | \hat{Q}_l^m | \Gamma'' \rangle \langle \Gamma'' | \hat{Q}_{l'}^{m'} | \Lambda' \rangle}{\epsilon''^2 + \omega^2} \tag{38} $$

and using Eq. 25 to relate the spherical multipole moment operators $\hat{Q}_l^m$ and $|\Lambda = \pm 1\rangle$ wavefunctions to their associated symmetrized components, $\hat{Q}_{l|m|}^{\pm}$ and $|(\Lambda = 1)^{\pm}\rangle$, where $\pm$ labels the parity by reflection through the $xz$ plane, we can relate the spherical components of the dynamic polarizability to the cartesian ones defined as

$$ {}^{pp'}\alpha_{lml'm'}^{qq'}(i\omega) = \sum_{\Gamma''} \frac{2\epsilon'' \langle \Lambda^p | \hat{Q}_{lm}^q | \Gamma'' \rangle \langle \Gamma'' | \hat{Q}_{l'm'}^{q'} | \Lambda'^{p'} \rangle}{\epsilon''^2 + \omega^2} \tag{39} $$

where $p, p', q, q' = \pm$ is the parity, and ${}^{pp'}\alpha_{lml'm'}^{qq'} = {}^{p'p}\alpha_{lml'm'}^{qq'}$. In the case of the dipole polarizability ($l = l' = 1$) associated with a diatom in a $\Pi$ state ($\Lambda = \pm 1$) we obtain the following relation between the spherical and cartesian components

$$ \begin{aligned} {}^{\Lambda\Lambda'}\alpha_{1m1m'}(i\omega) \;=\; & \frac{1}{4}\left[(1+\delta_{m0})(1+\delta_{m'0})\right]^{1/2} (-\sigma_\Lambda)^\Lambda (-\sigma_{\Lambda'})^{\Lambda'} (-\sigma_m)^m (-\sigma_{m'})^{m'} \\ & \times \Big\{ {}^{++}\alpha_{1m1m'}^{++}(i\omega) - \sigma_\Lambda\sigma_{\Lambda'}\sigma_m\sigma_{m'}(1-\delta_{m0})(1-\delta_{m'0})\, {}^{--}\alpha_{1m1m'}^{--}(i\omega) \\ & + \sigma_\Lambda\sigma_{\Lambda'}\, {}^{--}\alpha_{1m1m'}^{++}(i\omega) - \sigma_m\sigma_{m'}(1-\delta_{m0})(1-\delta_{m'0})\, {}^{++}\alpha_{1m1m'}^{--}(i\omega) \\ & + \left[\sigma_\Lambda\sigma_m(1-\delta_{m0}) - \sigma_{\Lambda'}\sigma_m(1-\delta_{m0})\right] {}^{+-}\alpha_{1m1m'}^{-+}(i\omega) \\ & + \left[\sigma_\Lambda\sigma_{m'}(1-\delta_{m'0}) - \sigma_{\Lambda'}\sigma_{m'}(1-\delta_{m'0})\right] {}^{+-}\alpha_{1m1m'}^{+-}(i\omega) \Big\} \end{aligned} \tag{40} $$

where $\sigma_\Lambda = \mathrm{sign}(\Lambda)$, $\sigma_m = \mathrm{sign}(m)$, and where it holds the following equalities ${}^{++}\alpha_{1010}^{++} = {}^{--}\alpha_{1010}^{++}$, ${}^{++}\alpha_{1111}^{++} = {}^{--}\alpha_{1111}^{--}$ and ${}^{++}\alpha_{1111}^{--} = {}^{--}\alpha_{1111}^{++}$ for a $\Pi$ diatom [10]. The present notation for cartesian components are related to that of Ref. [10] by

$$ \begin{aligned} {}^{++}\alpha_{1010}^{++} &= {}^{xx}\,\alpha_{1010}^{++}([10]) = {}^{xx}\,\alpha_{zz} \\ {}^{++}\alpha_{1111}^{++} &= {}^{xx}\,\alpha_{1111}^{++}([10]) = {}^{xx}\,\alpha_{xx} \qquad {}^{++}\alpha_{1111}^{--} = {}^{xx}\,\alpha_{1111}^{--}([10]) = {}^{xx}\,\alpha_{yy} \\ {}^{+-}\alpha_{1111}^{+-} &= {}^{xy}\,\alpha_{1111}^{+-}([10]) = {}^{xy}\,\alpha_{xy} \qquad {}^{+-}\alpha_{1111}^{-+} = {}^{xy}\,\alpha_{1111}^{-+}([10]) = {}^{xy}\,\alpha_{yx} \end{aligned} \tag{41} $$

[1] S.-H. Lee, K. Liu, Advances in Molecular Beam Research and Applications, edited by R. Campargue (Springer-Verlag, Berlin 2000).

[2] P. Casavecchia, Rep. Progr. Phys. **63**, 355 (2000).

[3] I.W.M. Smith, E. Herbst, Q. Chang, MNRAS **350**, 323 (2004).

[4] D. Carty, A. Goddard, S.P.K. Kohler, I.R. Sims, I.W.M. Smith, J. Phys. Chem. A **110**, 3101 (2006).

[5] A. Zanchet, B. Bussery-Honvault, P. Honvault, J. Phys. Chem. A, **110**, 12017 (2006).

[6] A. Zanchet, Ph. Halvick, J.-C. Rayez, B. Bussery-Honvault, P. Honvault, J. Chem. Phys. **126**, 184308 (2007).

[7] A. Zanchet, Ph. Halvick, B. Bussery-Honvault, P. Honvault, J. Chem. Phys. **128**, 204301 (2008).

[8] M.M. Graff, A.F. Wagner, J. Chem. Phys. **92**, 2423 (1990).

[9] P.E.S. Wormer, J.A. Klos, G.C. Groenenboom, A. Van der Avoird, J. Chem. Phys. **122**, 244325 (2005).

[10] D. Spelsberg, J. Chem. Phys. **111**, 9625 (1999).

[11] A.V. Fishchuk, P.E.S. Wormer, A. van der Avoird, J. Phys. Chem. A, **110**, 5273.

[12] W.B. Zeimen, J. Klos, G.C. Groenenboom, A. van der Avoird, J. Chem. Phys. **118**, 7340.

[13] M.M. Graff, ApJ **339**, 239 (1989).

[14] A.I. Maergoiz, E.E. Nikitin, J. Troe, V.G. Ushakov, in "Theory of Chemical Reaction Dynamics", Ed. A. Lagana anf G. Lendvay, Kluwer Academic Publishers, Dordrecht, ISBN: 978-1402020551, (2004).

[15] MOLPRO, a package of *ab initio* programs designed by H.-J. Werner P. J. Knowles, version 2002.6, R. D. Amos, A. Bernhardsson, A. Berning, P. Celani, D. L. Cooper, M. J. O. Deegan, A. J. Dobbyn, F. Eckert, C. Hampel, G. Hetzer, P. J. Knowles, T. Korona, R. Lindh, A. W. Lloyd, S. J. McNicholas, F. R. Manby, W. Meyer, M. E. Mura, A. Nicklass, P. Palmieri, R. Pitzer, G. Rauhut, M. Sch´utz, U. Schumann, H. Stoll, A. J. Stone, R. Tarroni, T. Thorsteinsson, H.-J. Werner.

[16] A. Zanchet et al. (in preparation).

[17] W.R. Gentry, C.F. Giese, J. Chem. Phys. **67**, 2355 (1977).

[18] D. Spelsberg, T. Lorenz, W. Meyer, J. Chem. Phys. **99**, 7845 (1993).

[19] K.I. Peterson, G.T. Fraser, W. Klemperer, Can. J. Phys. **62**, 1502 (1984).

[20] D.D. Nelson, A. Schiffman, D.J. Nesbitt, J.J. Orlando, J.B. Burkholder, J. Chem. Phys. **93**, 7003 (1990).

[21] K. Andersson, A.J. Sadlej, Phys. Rev. **46**, 2356 (1992).

[22] K. Schröder, V. Staemmler, M.D. Smith, D.R. Fowler, J. Jaquet, J. Phys. B, **24**, 2487 (1991).

[23] A. Beghin, T. Stoecklin, J.C. Rayez, Chem. Phys. **195**, 259 (1995).

[24] M. Rérat, B. Bussery, M. Frécon, J. Mol. Spectr. **182**, 260 (1997).

[25] D. Spelsberg and W. Meyer, J. Chem. Phys., **108**, 1532 (1998).

[26] S.P. Karna, J. Chem. Phys. **104**, 6590 (1996).

[27] P.W. Fowler, P. Jørgensen and J. Olsen, J. Chem. Phys. **93**, 7256 (1990).

[28] "DALTON, a molecular electronic structure program, Release 2.0 (2005), see http://www.kjemi.uio.no/software/dalton/dalton.html "

[29] P.W. Langhoff, M. Karplus, J. Chem. Phys. **53**, 233 (1970).

[30] X. Chu, A. Dalgarno, G.C. Groenenboom, Phys. Rev. A, **72**, 032703 (2005).

[31] G.C. Nielson, G.A. Parker, R.T. Pack, J. Chem. Phys. **64**, 2055 (1976).

[32] M.E. Rose, in *Elementary theory of angular momentum*, Dover Inc., NY, 1995.

[33] M.W. Chase, J.L. Curnutt, J.R. Downey, R.A. McDonald, A.N. Syverud, E.A. Valenzuela, J. Phys. Chem. Ref. Data **11**, 695 (1982).

[34] National Institute of Standards and Technology, http://www.nist.gov/

TABLE I: Static multipole moments (in atomic units) for C($^3P$) and OH($X^2\Pi$).

| | C($^3P$) | OH($X^2\Pi$) |
|---|---|---|
| $Q_1^0$ | | 0.651[a,b], 0.64628[c] |
| | | 0.6545[d], 0.6512[e] |
| $Q_2^0$ | +1.539[f], +1.42[g],+1.397[h] | 1.35[a], 1.30827[c] |
| | +1.556[i],-1.426[j] | 1.3939[d] |
| $Q_2^{\pm 2}$ | | -1.070[a], -0.85941[c], -1.1825[d] |
| $Q_2^{\pm 2}$(GW)[k] | | -5.24[a], -4.21[c], -5.79[d] |

[a]Ref. [13]; [b]Experimental value: Ref. [19]; [c]Ref. [10]; [d]Ref. [9]; [e]Ref. [20]; [f] RHF value (small CASSCF) of Ref.[21]; [g]CASSCF value of Ref. [21]; [h]Ref. [22]; [i]Ref. [23]; [j]Ref. [24]; [k]Values with the convention of Graff and Werner, as given by Eq. (8).

TABLE II: Static and dynamic dipole polarizabilities (in $a_0^3$) for C($^3P$) and OH($X^2\Pi$).

| | C($^3P_{zz}$) | | | OH($X^2\Pi$) | | | |
|---|---|---|---|---|---|---|---|
| $\omega$ | $\alpha_{zz}$ | $\alpha_{xx}$ | $\omega$ | $^{xx}\alpha_{zz}$ | $^{xx}\alpha_{xx}$ | $^{xx}\alpha_{yy}$ | $<\alpha>$ |
| 0.0 | 10.264[a], 9.62[b] | 12.396[a], 11.6[b] | | 8.751[c] | 6.374[c] | 7.554[c] | 7.557 [c] |
| | 9.82/9.95[d] | 11.92/12.11[d] | | 8.70[a] | 6.26[a] | 7.65[a] | 7.54[a],7.053[e] |
| | 10.59/9.98[e] | 12.12/12.80[e] | | | | | |
| $\omega$ | $\alpha^f_{zz}$ | $\alpha^f_{xx}$ | $\omega$ | $^{xx}\alpha^g_{zz}$ | $^{xx}\alpha^g_{xx}$ | $^{xx}\alpha^g_{yy}$ | |
| 0.1 | 9.799 | 11.603 | 0.5 | 5.408 | 4.200 | 4.448 | |
| 0.2 | 8.675 | 9.847 | 1.0 | 2.886 | 2.512 | 2.527 | |
| 0.3 | 7.353 | 8.018 | 1.5 | 1.724 | 1.554 | 1.558 | |
| 0.4 | 6.122 | 6.484 | 2.0 | 1.120 | 1.018 | 1.024 | |
| 0.5 | 5.084 | 5.283 | 2.5 | 0.775 | 0.706 | 0.712 | |
| 0.6 | 4.242 | 4.358 | 3.0 | 0.564 | 0.513 | 0.520 | |
| 0.7 | 3.570 | 3.642 | 3.5 | 0.427 | 0.388 | 0.394 | |
| 0.8 | 3.032 | 3.082 | 4.0 | 0.334 | 0.303 | 0.308 | |
| 0.9 | 2.600 | 2.637 | 4.5 | 0.267 | 0.243 | 0.247 | |
| 1.0 | 2.250 | 2.280 | 5.0 | 0.219 | 0.199 | 0.202 | |

[a] Linear response values of present work; [b]Ref. [24]; [c] Ref. [10]; [d]CASSCF and averaged CASPT2 values of Ref. [21]; [e]TDUHF and ROHF-FF values of Ref. [26] at $r_0^{OH} = 1.95a_0$; [f]evaluated from [10,9] Padé approximants obtained from Cauchy moments; [g]obtained from OH pseudo-spectra of Ref. [10] calculated at $r_0^{OH} = 1.865a_0$.

TABLE III: Long-range non zero ${}^{ii'jj'}V_{4L_bM_aM_b}$ and ${}^{ii'jj'}V_{5L_bM_aM_b}$ electrostatic coefficients (in atomic units) for the C($^3P$) + OH($X^2\Pi$) interaction.

| $LM_L$ | $L'M'_L$ | $\Lambda\Lambda'$ | $M_a$ | $M_b$ | $L_b$ | ${}^{ii'jj'}V_4^{\rm elec}$ | $M_a$ | $M_b$ | $L_b$ | ${}^{ii'jj'}V_5^{\rm elec}$ |
|---|---|---|---|---|---|---|---|---|---|---|
| $\pm1$ | $\pm1$ | $\pm1\pm1$ | 0 | 0 | 1 | -1.5199 | 0 | 0 | 2 | -6.5067 |
| $\pm1$ | 0 | $\pm1\pm1$ | -1 | 0 | 1 | 1.5199 | -1 | 0 | 2 | 7.5133 |
| $\pm1$ | $\mp1$ | $\pm1\pm1$ | -2 | 0 | 1 | 0.000 | -2 | 0 | 2 | -2.6564 |
| 0 | $\pm1$ | $\pm1\pm1$ | 1 | 0 | 1 | -1.5199 | 1 | 0 | 2 | -7.5133 |
| 0 | 0 | $\pm1\pm1$ | 0 | 0 | 1 | 3.0398 | 0 | 0 | 2 | 13.013 |
| $\pm1$ | $\pm1$ | $\pm1\mp1$ | | | | | 0 | 2 | 2 | 5.5199 |
| $\pm1$ | 0 | $\pm1\mp1$ | | | | | -1 | 2 | 2 | -6.3738 |
| $\pm1$ | $\mp1$ | $\pm1\mp1$ | | | | | -2 | 2 | 2 | 2.2535 |
| 0 | $\pm1$ | $\pm1\mp1$ | | | | | 1 | 2 | 2 | 6.3738 |
| 0 | 0 | $\pm1\mp1$ | | | | | 0 | 2 | 2 | -11.0398 |

TABLE IV: Long-range non zero ${}^{ii'jj'}V_{6L_bM_aM_b}$ dispersion and induction coefficients (in atomic units) for the C($^3P$) + OH($X^2\Pi$) interaction.

| $M_L$ | $M'_L$ | $\Lambda\Lambda'$ | $M_a$ | $M_b$ | $L_b$ | ${}^{ii'jj'}V_6^{\rm disp}$ | $M_L$ | $M'_L$ | $\Lambda\Lambda'$ | $M_a$ | $M_b$ | $L_b$ | ${}^{ii'jj'}V_6^{\rm ind}$ |
|---|---|---|---|---|---|---|---|---|---|---|---|---|---|
| $\pm1$ | $\pm1$ | $\pm1\pm1$ | 0 | 0 | 0 | -36.529 | -1 | -1 | $\pm1\pm1$ | 0 | 0 | 0 | -5.106 |
| $\pm1$ | $\pm1$ | $\pm1\pm1$ | 0 | 0 | 2 | -2.871 | -1 | -1 | $\pm1\pm1$ | 0 | 0 | 2 | -5.407 |
| $\pm1$ | 0 | $\pm1\pm1$ | -1 | 0 | 2 | 0.168 | -1 | 0 | $\pm1\pm1$ | -1 | 0 | 2 | 0.522 |
| $\pm1$ | $\mp1$ | $\pm1\pm1$ | -2 | 0 | 2 | -0.119 | -1 | 1 | $\pm1\pm1$ | -2 | 0 | 2 | -0.369 |
| 0 | $\pm1$ | $\pm1\pm1$ | 1 | 0 | 2 | -0.168 | 0 | -1 | $\pm1\pm1$ | 1 | 0 | 2 | -0.522 |
| 0 | 0 | $\pm1\pm1$ | 0 | 0 | 0 | -34.737 | 0 | 0 | $\pm1\pm1$ | 0 | 0 | 0 | -4.654 |
| 0 | 0 | $\pm1\pm1$ | 0 | 0 | 2 | -2.435 | 0 | 0 | $\pm1\pm1$ | 0 | 0 | 2 | -4.051 |
| $\pm1$ | $\pm1$ | $\pm1\mp1$ | 0 | $\pm2$ | 2 | -1.532 | | | | | | | |
| $\pm1$ | 0 | $\pm1\mp1$ | -1 | $\pm2$ | 2 | 0.109 | | | | | | | |
| $\pm1$ | $\mp1$ | $\pm1\mp1$ | -2 | $\pm2$ | 2 | -0.077 | | | | | | | |
| 0 | $\pm1$ | $\pm1\mp1$ | 1 | $\pm2$ | 2 | -0.109 | | | | | | | |
| 0 | 0 | $\pm1\mp1$ | 0 | $\pm2$ | 2 | -1.248 | | | | | | | |

**FIGURES CAPTIONS**

FIGURE 1. Electrostatic plus induction (continuous line) or electrostatic only (dashed line) potential energies (in $cm^{-1}$) for the 12 non-relativistic long-range $C(^3P)$ + $OH(X^2\Pi)$ states as a function of the intermolecular distance R (in bohr) for linear geometries of the complex. The long-range multipolar potentials are compared with previous *ab initio* CASSCF calculations. (a)$\gamma$=0°: $X^2A'(^2\Sigma^+)$(circle), $2^2A' - 1^2A''(^2\Delta)$(square), $2^2A''(^2\Sigma^-)$(cross), $3^2A' - 3^2A''(^2\Pi)$(triangle); (b)$\gamma$=180°: ($X^2A' - 1^2A''(^2\Pi)$(square), $2^2A'(^2\Sigma^+)$(circle), $3^2A' - 2^2A''(^2\Delta)$(triangle), $3^2A''(^2\Sigma^-)$(cross).

FIGURE 2. Electrostatic plus induction (continuous line) or electrostatic only (dashed line) potential energies (in $cm^{-1}$) for the 12 non-relativistic long-range $C(^3P)$ + $OH(X^2\Pi)$ states as a function of the OH bending angle, $\gamma$ (in degree) at intermolecular distance, R=25 bohr. The long-range multipolar potentials are compared with previous *ab initio* CASSCF calculations: $X^2A'(^2\Sigma^+ -^2 \Pi)$(square), $2^2A'(^2\Delta -^2 \Sigma^+)$(circle), $3^2A'(^2\Pi -^2 \Delta)$(triangle up), $1^2A''(^2\Delta -^2 \Pi)$(diamond), $2^2A''(^2\Sigma^- -^2 \Delta)$(triangle down), $3^2A''(^2\Pi -^2 \Sigma^-)$(cross).

FIGURE 3. Full (electrostatic + induction + dispersion) multipolar potential energies (in $cm^{-1}$ ) including monomer spin-orbit splittings for the 18 long-range $C(^3P)$ + $OH(X^2\Pi)$ states as a function of the intermolecular distance R (in bohr) at (a) $\gamma$=0° and (b)$\gamma$=180°. States are characterized by their $\Omega$ value: $\frac{7}{2}$(continuous), $\frac{5}{2}$(dotted), $\frac{3}{2}$(dot-dashed) or $\frac{1}{2}$ (short dashed).

FIGURE 4. Full (electrostatic + induction + dispersion) multipolar potential energies (in $cm^{-1}$) including monomer spin-orbit splittings for the 18 long-range $C(^3P)$ + $OH(X^2\Pi)$ states as a function of the OH bending angle, $\gamma$ (in degree) at intermolecular distance, R=10 bohr.

Figure 1a: Bussery-Honvault et al.

Figure 1b: Bussery-Honvault et al.

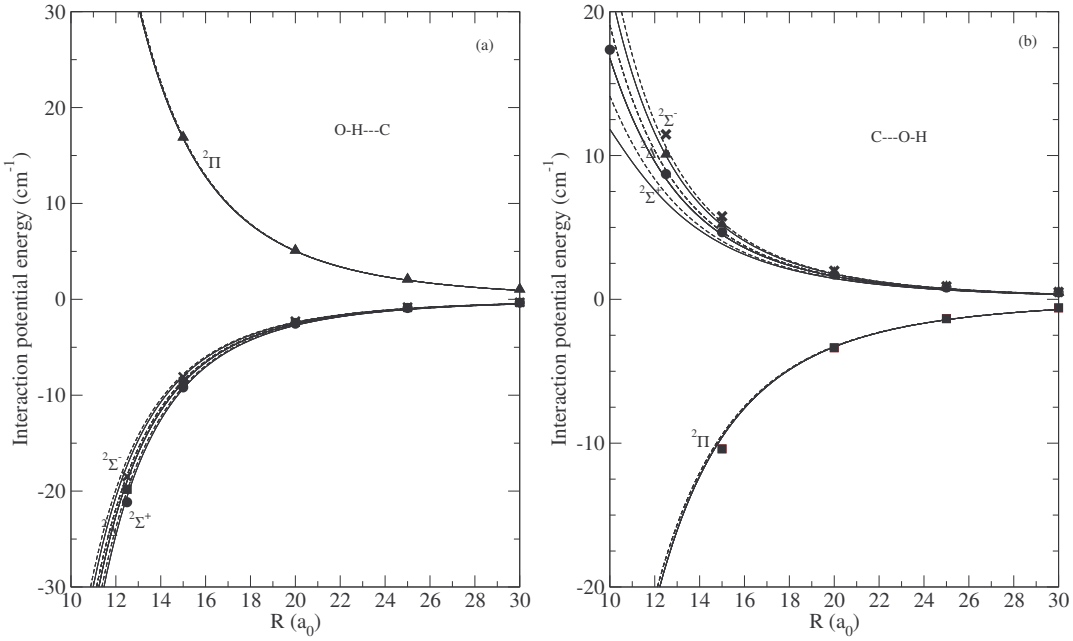


FIG. 1:

Figure 2: Bussery-Honvault et al.

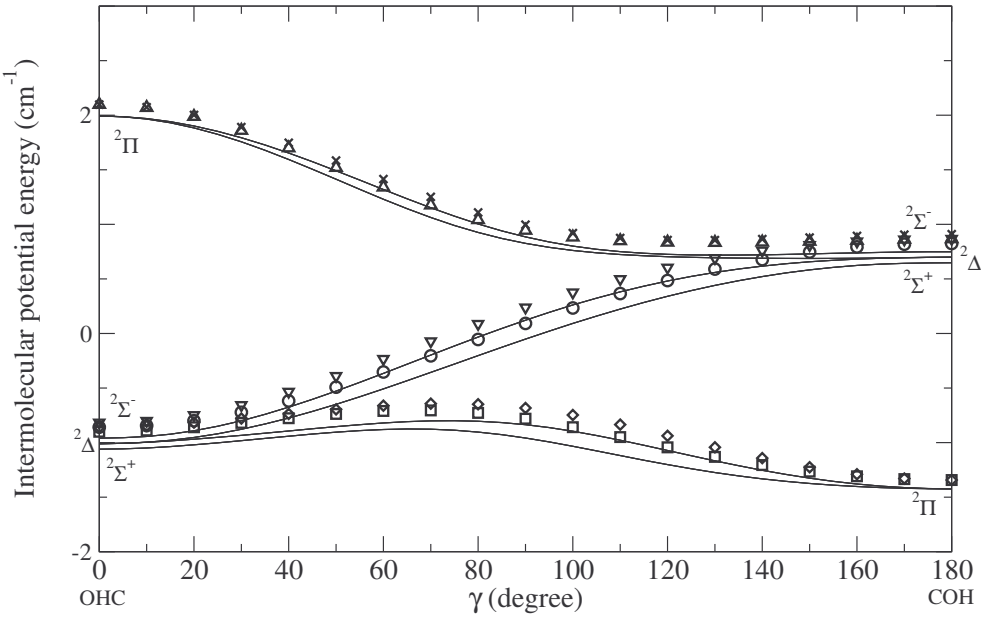


FIG. 2:

Figure 3a: Bussery-Honvault et al.

Figure 3b: Bussery-Honvault et al.

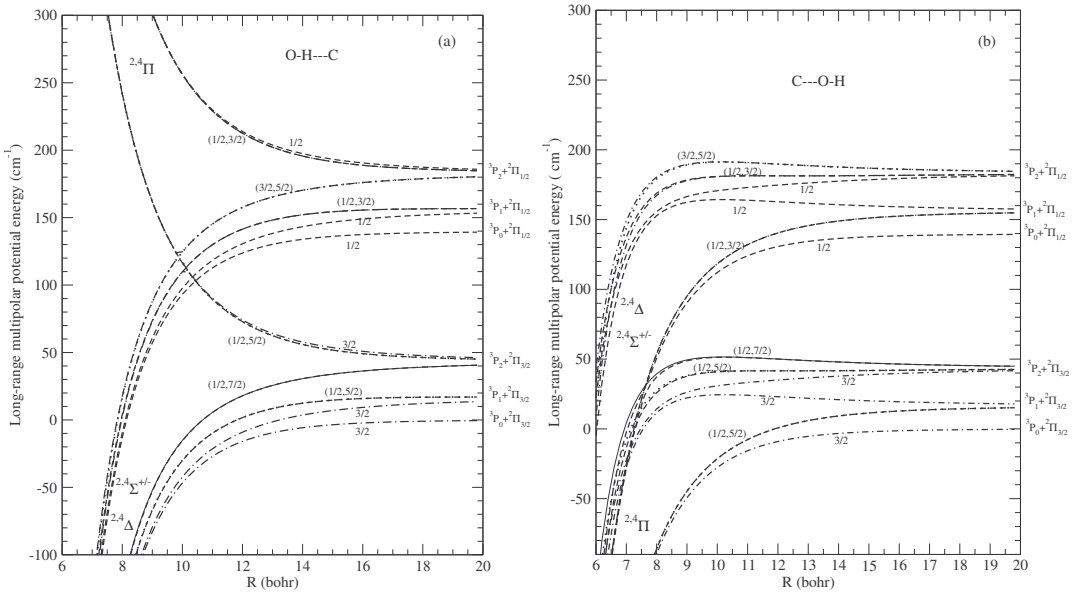


FIG. 3:

Figure 4: Bussery-Honvault et al.

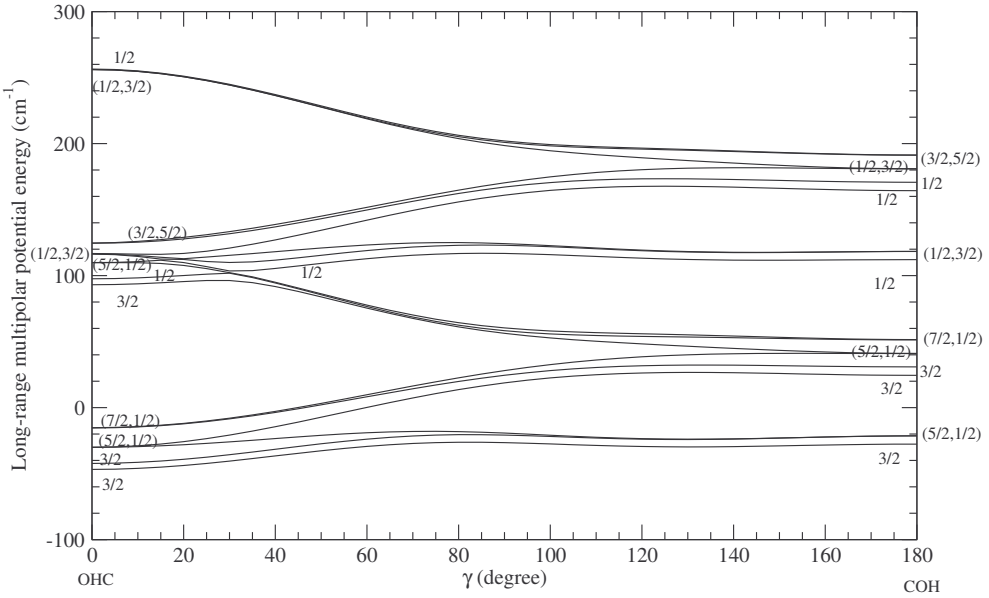


FIG. 4: